Journal of Applied Polymer Science

Morphological Evolution and Properties of Thermoplastic Vulcanizate/Organoclay Nanocomposites

Chaoqun Li,[1] Zhiwei Jiang,[2] Tao Tang[2]

[1]Key Laboratory for Advanced Materials in Tropical Island Resources, Ministry of Education, College of Materials and Chemical Engineering, Hainan University, Haikou 570028, People's Republic of China

[2]State Key Laboratory of Polymer Physics and Chemistry, Changchun Institute of Applied Chemistry, Chinese Academy of Sciences, Changchun 130022, People's Republic of China

Correspondence to: T. Tang (E-mail: ttang@ciac.jl.cn)

ABSTRACT: Nanocomposites composed of organoclay and thermoplastic vulcanizates (TPVs) based on uncompatibilized or compatibilized polypropylene (PP)/ethylene–propylene–diene rubber (EPDM) blends were prepared in this study. The morphology of the nanocomposites was studied with wide-angle X-ray diffraction and transmission electron microscopy, which suggested that the addition of the compatibilizer played a key role in determining the morphology of the composites because of their interaction with the clay surface. Scanning electron microscopy study indicated the changes in the morphology of the rubber particles. Dynamic mechanical analysis was also applied to the analysis of these phenomena. Moreover, for nanocomposites with uncompatibilized PP/EPDM blends as the matrix, the samples showed tensile enhancement compared with neat TPV. Although the addition of the compatibilizer changed tensile properties of the composites in a rather different trend, the tensile modulus increased dramatically when the compatibilizer was added. © 2014 Wiley Periodicals, Inc. J. Appl. Polym. Sci. **2014**, *131*, 40618.

KEYWORDS: clay; crosslinking; elastomers

Received 26 December 2013; accepted 17 February 2014
DOI: 10.1002/app.40618

INTRODUCTION

Thermoplastic elastomer compositions based on uncured olefinic elastomer components are referred to as *thermoplastic olefins* (TPOs). The addition of a small quantity of curing agents during melt mixing leads to the *in situ* vulcanization of the rubber component, which produces thermoplastic vulcanizates (TPVs).[1,2] TPVs have gained significant attention because of their outstanding processing and physical properties.[3–7]

Nanofillers, such as organoclays, possess excellent mechanical and thermal properties because of their unique structure; they have shown much potential in the reinforcement of polymer matrices.[8,9] It is generally accepted that the properties of prepared materials are significantly influenced by the dispersion and distribution of clay in the polymer matrix. Much work that has been done has dealt with the morphology of TPO/clay nanocomposites with maleated polypropylene (PPMA) or maleated rubber as a compatibilizer,[10–14] although other studies have shown that the blending process is very important and affects the morphology and final properties of the composites.[15,16] For example, Lee and Goettler[16] introduced clay to strengthen TPO and found that the dispersion and distribution state of the clay could be controlled through changes in the blending sequence.

There have also been a few investigations that have been carried out to strengthen TPVs with clay.[16–21] Their study showed that it was impossible for clay to disperse into the dispersed rubber phase when the rubber particles were crosslinked in advance of the addition of the clay.[16,21] To date, there have been few works on the study of the *in situ* strengthening of dynamically vulcanized TPOs with clay.[18–21] Naderi et al.[19] studied the microstructure–property correlation for thermoplastic vulcanizate nanocomposites (TPVNs) with PPMA as a compatibilizer, and the results show that the tensile modulus of the TPVNs increased, whereas organoclay acted as a nucleating agent and improved the properties of the TPVs. It was also reported that the presence of nanoclay affected the crosslinking reaction through its barrier effect, which affected the cocontinuity of the components.[20] However, systematic investigations to illustrate the morphology evolutions and properties of TPVNs are still needed.

The purpose of this study was to examine the relation between the phase structure and mechanical properties of prepared TPV-based nanocomposites. The dispersion and distribution of

Table I. Compositions of the TPV/Organoclay Nanocomposites

Sample code	PP/EPDM	OMMTs	PPMA
TPV	100		
TPVN1	99	1	
TPVN2.5	97.5	2.5	
TPVN5	95	5	
TPVN10	90	10	
TPVN5 (two-step)	95	5	

organoclay were examined for systems with no compatibilizer or with PPMA as a compatibilizer. Furthermore, the effect of the organoclay on the mechanical properties of the composites was also studied.

EXPERIMENTAL

Materials

Ethylene–propylene–diene rubber (EPDM), with ethylidene norbornene as a termonomer, with an ethylene content of about 70 wt %, was supplied by DuPont–Dow Elastomers [Mooney viscosity = 70, ML(1+4), 100°C]. The isotactic polypropylene (PP; melt flow index = 0.8 at 190°C and 5 kg) used in this study was supplied by Panjin Chemical Co. PPMA was supplied by Sanyo Chemical Industries. The acid value of PPMA was 26 mg of KOH/g. Phenolic resin (SP-1045), in combination with stannous chloride ($SnCl_2$), was used as the curing agent. Na^+ montmorillonites (MMTs) with cation-exchange capacities (CECs) of 119 mequiv/100 g were supplied by Kunimine Co. Octadecylamine was used as a precursor of the modifier and was supplied by Wako Pure Chemical Industries Co.

Cation Exchange

Organically modified montmorillonites (OMMTs) were synthesized by a cation-exchange reaction, as described in our previous article.[22] Octadecylammonium chloride (octadecylamine protonated with equimolar concentrated HCl in deionized water at 80°C) as a modifier was poured into a hot dispersion of MMT. The mixtures was stirred vigorously for 30 min, washed with deionized water at 80°C, and finally dried. The loading level of the modifier with respect to the CEC (mequiv/g) was 100%.

Fabrication of the TPV/Organoclay Nanocomposites

We carried out the compounding by first mixing PP with EPDM for 2 min; then, organoclay was added, and the blending was conducted for another 10 min. In the final step, the curing system was added, and the mixing was continued until a constant value of torque was obtained. The absolute contents of the curing agent were kept constant in this study. The dynamically vulcanized composites were taken out and sheeted through a two-rolled mill and were then cut into pieces. The prepared composites were then compression-molded under a pressure of 10 MPa at 180°C; this was followed by cold compression for 8 min. In addition, neat TPV was prepared under the same conditions for comparison.

For the first set, the organoclay was filled in the EPDM/PP blends (where the EPDM/PP weight ratio was kept constant at 70:30), and then, the system was dynamically crosslinked. The recipe showed the variation in the concentration of the organoclay (shown in Table I, here the numbers after TPVN refer to the content of OMMT by weight.) and the vulcanizing system on the basis of 100 phr EPDM, 1.5 phr SP-1045, and 1 phr $SnCl_2$. A sample was also prepared with a two-step processing method in which the EPDM and organoclay were first mixed for 8 min to obtain a masterbatch, and then, the masterbatch was melt-blended with PP for another 3 min.

For the second set of samples, PPMA was introduced to improve the dispersion of the organoclay, and the weight ratio of PPMA to organoclay was fixed at 3:1, whereas the EPDM/PP weight ratio was kept constant at 80:20. (When the polymeric compatibilizer PPMA was added to a composite, the content of the EPDM/PP with 80:20 was reduced by the amount of the compatibilizer.) EPDM, PP, and PPMA were added simultaneously, whereas the other blending procedures were done in the order described previously.

Characterization

Wide-angle X-ray diffraction (WAXD) was carried out with a Rigaku model Dmax 2500 with a Cu Kα radiation, and the interlayer distances (d_{001}'s) of MMT were estimated from the (001) peaks in the WAXD patterns with Bragg's formula.

The morphologies of the composites were observed by transmission electron microscopy (TEM; JEOL2010) on microtome sections of the nanocomposites. Ultrathin sections were cryogenically cut at −40°C with a Leica Ultracut instrument. The sections were stained by RuO_4 vapor.

Scanning electron microscopy (SEM; model XL30E, Japan) experiments were carried out to examine the morphologies of the samples. The fractured surfaces of the samples were etched with hot xylene for 30 s and sputter-coated with gold.

The static mechanical properties were measured with an Instron 1121 tensile testing machine, and the crosshead rate was set at 50 mm/min. For each data point, five samples were tested, and the average value was taken.

Dynamic mechanical analysis of samples was carried out with a dynamic mechanical analyzer (DMA242C) in tension mode with the following parameters: frequency = 1 Hz, scanning rate = 3°C/min, and temperature range = −100 to 100°C.

RESULTS AND DISCUSSION

Torque versus Time

Figure 1 compares the curing behavior of samples consisting of various amount of organoclay. It shows that the curing characteristics of the samples were influenced by the organoclay filler. After the organoclay was added, the samples exhibited a lower mixing torque level. We also observed the phenomenon of retardation in the crosslinking reaction with increasing organoclay loadings; similar results were reported for rubber/organoclay systems.[23,24] These could be ascribed to the absorption of the phenolic curing system on the active surface of the OMMTs and the possible reaction of the hydroxyl groups of the phenolic resin with the octadecylamine-modified MMTs. In addition, fillers such as silica or carbon black could also absorb the curing

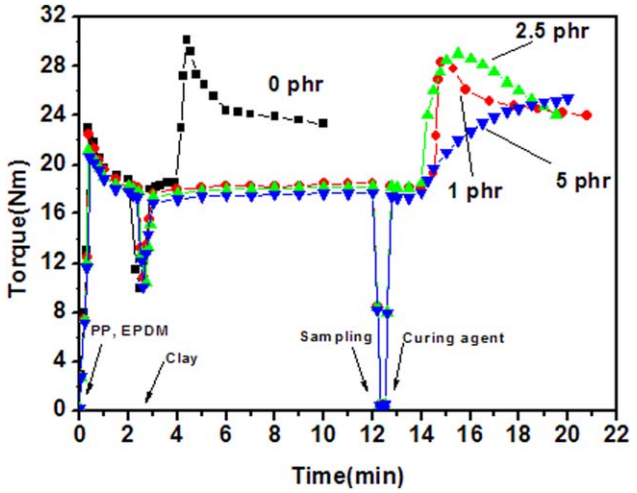

Figure 1. Torque versus time for the uncompatibilized TPVNs with OMMT contents of (a) 0, (b) 1, (c) 2.5, and (d) 5 wt %. [Color figure can be viewed in the online issue, which is available at wileyonlinelibrary.com.]

agents and decrease the crosslinking density of TPV composites, as previously reported in some studies.[25,26]

To further understand the morphology of the TPVNs, PPMA was used as a compatibilizer during the mixing of the organoclay with PP/EPDM. The curing of EPDM is shown in Figure 2. It shows that value of MH-ML(the highest torque (MH) subtracting the lowest torque (ML)) in the TPVNs was the same as the one without organoclay. This meant that the phenolic resin curing agents were not adsorbed on the surface of the OMMTs; thus, the crosslink density of the TPVNs was not affected by the addition of organoclay; this was different from the TPV series without compatibilizer. Also, the crosslinking reaction of the TPVNs was retarded.

WAXD of the Organoclay and Prepared Nanocomposites

Figure 3 shows the WAXD scans for the organoclay and uncompatibilized TPVNs. The OMMTs showed an intense peak

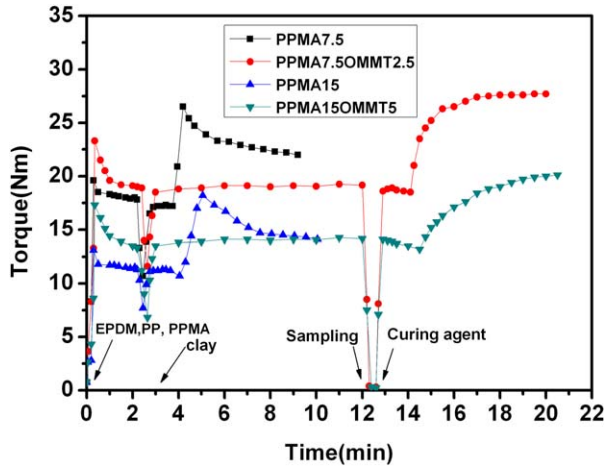

Figure 2. Torque versus time for the compatibilized TPVNs (The numbers after "PPMA" and "OMMT" represent the content of each component by weight, for example, PPMA7.5OMMT2.5 denotes the sample contains 7.5 wt% PPMA and 2.5 wt%OMMT.). [Color figure can be viewed in the online issue, which is available at wileyonlinelibrary.com.]

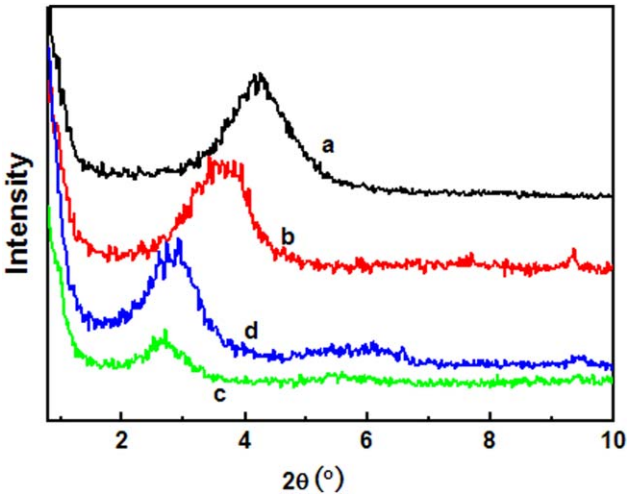

Figure 3. X-ray diffraction patterns of the organoclay and TPVNs (uncompatibilized series): (a) OMMTs, (b) TPON5 (the counterpart of TPVN5 but unvulcanized), (c) TPVN2.5, and (d) TPVN5. [Color figure can be viewed in the online issue, which is available at wileyonlinelibrary.com.]

around $2\theta = 4.26°$ corresponding to a d_{001} of 20.7 Å. The d_{001}'s of the OMMTs in TPONT5 (TPON is the unvulcanized counterpart of TPVN, and the numbers after TPON represent the content of OMMTs by weight) increased to 2.7 nm. For TPVNs, the d_{001} peak of the OMMTs shifted to a lower angle, and the d_{001}'s increased to 3.3 and 3.0 nm for TPVN2.5 and TPVN5, respectively. The WAXD results suggested that the d_{001}'s of the OMMTs become larger after melt mixing with the PP/EPDM blends, whereas the d_{001}'s of the OMMTs increased further during dynamic vulcanization. In summary, the X-ray scans indicated that an intercalated structure of the TPVNs was developed because of the nonpolar nature of the PP/EPDM blends; it was rather difficult to obtain an exfoliate structure.[16] However, the

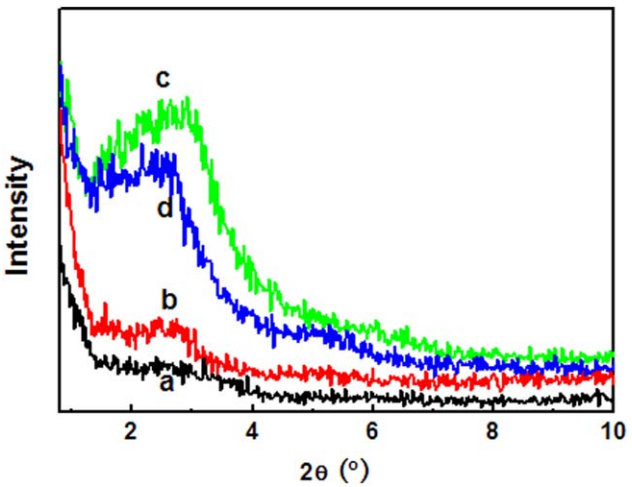

Figure 4. X-ray diffraction patterns of the TPONs (the counterparts of TPVNs but unvulcanized) and TPVNs (the compatibilized series): (a) TPON2.5, (b) TPVN2.5, (c) TPON5, and (d.) TPVN5. [Color figure can be viewed in the online issue, which is available at wileyonlinelibrary.com.]

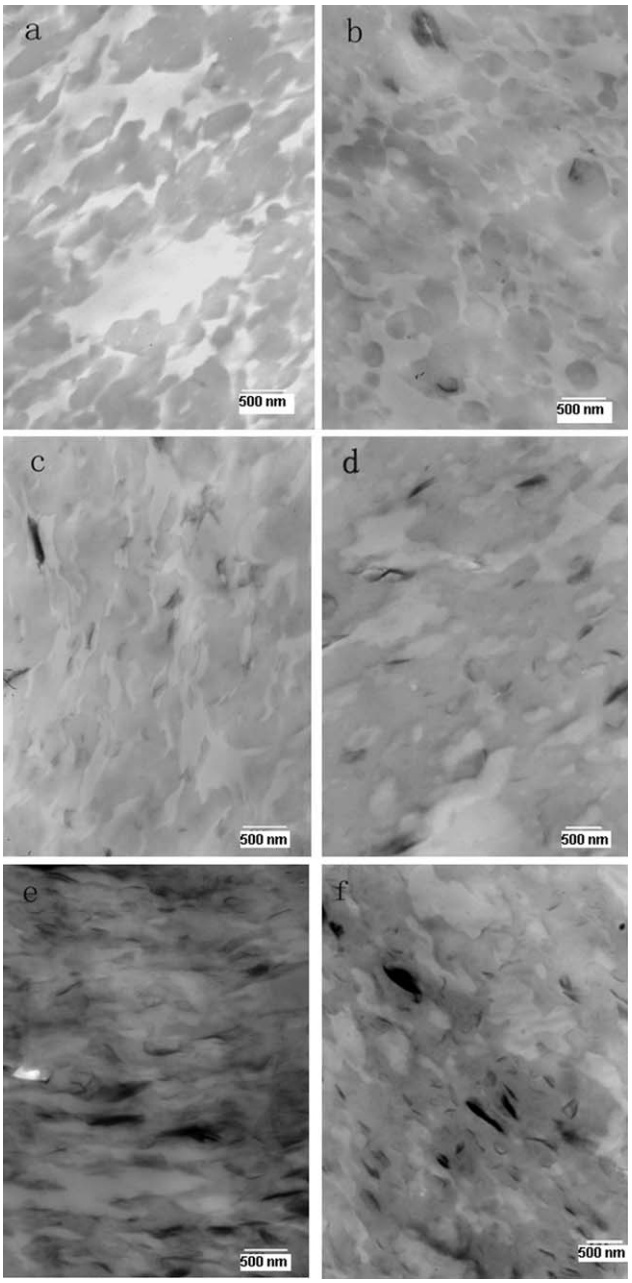

Figure 5. TEM micrographs of the TPVNs (the uncompatibilized series): (a) TPV, (b) TPVN1, (c) TPVN2.5, (d) TPVN5, (e) TPVN10, and (f) TPVN5 (two-step).

obviously increase in the d_{001}'s of OMMTs demonstrated that the compatibility between the matrix and organoclay was improved by dynamic vulcanization. These effects may have been derived from the reaction between the hydroxyl group of the phenolic resin and the surfactant of OMMT as the surfactant containing primary amine modifiers. Thus, the reaction of the curing agent with the active surface of the OMMT had a dominant influence on the intercalation and exfoliation of the clay,[23,27,28] as has been reported in other works.

Figure 4 shows the d_{001}'s of the OMMTs within the TPVNs containing compatibilizer. We observed that vulcanization had no effect on the increase of the d_{001}'s of the OMMTs; this indicated that the increase in the viscosity and shear stress during vulcanization did not help the intercalation of the polymer molecular chain into the organoclay interlayer. Generally, both the compatibility of a polymer with organoclay and the applied shear stress have a profound influence on the d_{001}'s of OMMTs.[8] In this study, the influence of the shear stress during vulcanization seemed not to be the main factor affecting the increase of the d_{001}'s of OMMTs. This result indirectly proved that the increase in the d_{001}'s of the OMMTs for the uncompatibilized TPVNs was due to the improvement in compatibility during vulcanization.

Morphological Characterization with TEM and SEM

Figure 5 shows the TEM micrographs for the TPV and TPVNs (uncompatibilized series), where the black lines represent the clay cross sections. Most of the organoclay still maintained ordered stacks (tactoid); clay stacks with a thickness of about a few tens of nanometers were dispersed in the TPV matrix uniformly. Moreover, rubber particles were dispersed in the continuous PP matrix in both the TPV and TPVNs, which showed typical TPV characteristics.

Figure 5(c,d) clearly shows that most of the organoclays were distributed in the rubber phase or in the interface of the two phases. It has been reported that for polymer blends that have distinct difference in polarity, clay is preferentially distributed in the more polar phase.[10–12] For unvulcanized nonpolar blends, such as PP/EPDM systems, clay would be uniformly distributed in both phases.[16] In this study, because of the vulcanization of the rubber phase, it became more polar and showed much stronger interaction with the active groups on the surface of the OMMTs compared to those on the surface of PP; this contributed to the variation in the distribution of the organoclay in the components of the dynamically vulcanized samples.[25,26] Figure 5(f) shows the morphology of the TPVN prepared by a two-step processing method; the clay plates were dominantly distributed in rubber phase. This indicated that the mixing sequence had a profound influence on the distribution of the organoclay. When the organoclay was first blended with EPDM, it preferred to stay in the rubber phase; for the TPVN5 prepared with the two-step processing method, most of the organoclay plates remained in the rubber phase after PP was added, and the morphology was fixed after vulcanization. This result provided guidance for us to control the distribution of the organoclay in a special phase.

As shown in Figure 5, we also observed a dramatic change in the morphology of the rubber phase with increasing organoclay content. For example, the rubber particles seemed to be more elongated. For the TPVNs containing 10 wt % OMMTs, the change in the morphology of the rubber particles was even more pronounced. Moreover, the addition of organoclay increased the size of the rubber particles, and some of the rubber particles even interconnected with one another. The morphological evolutions of the nanocomposites were proven by SEM (Figure 6). With increasing organoclay loading, rubber the particles interconnected with one another, and TPVN5 showed a cocontinuous morphology.[20] As the migration of the organoclay into the rubber phase changed the viscosity ratio of the

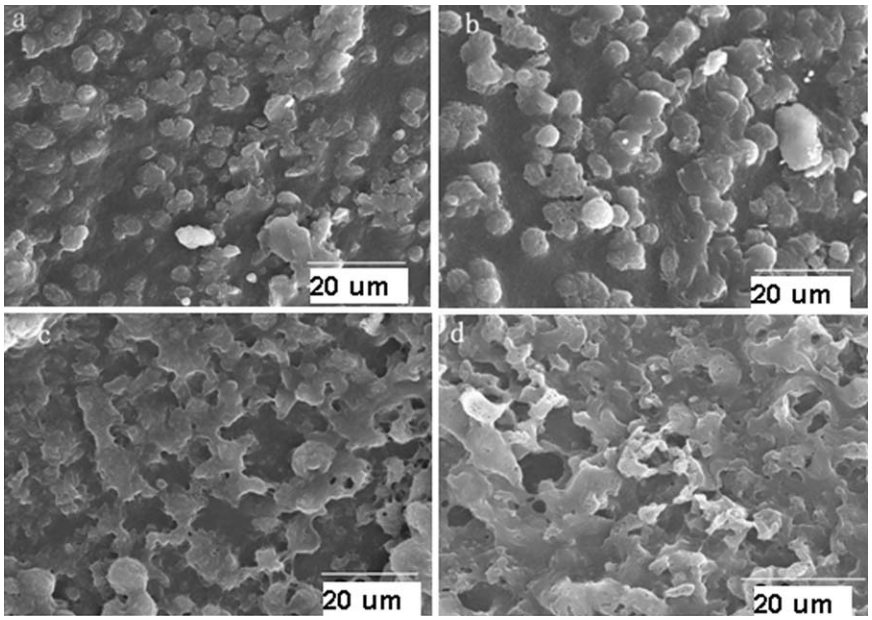

Figure 6. SEM images of TPVNs (the uncompatibilized series): (a) TPV, (b) TPVN1, (c) TPVN2.5, and (d) TPVN5.

two phases, the rubber particles stiffened more, and their deformability decreased during vulcanization; this led to the morphological evolution of the samples. A similar observation was also found by Naderi and coworkers.[19,26] Moreover, in this study, the reduction in the torque of the TPVNs on the influence of the rubber morphology was not excluded.

Figure 7 compares the TEM micrographs of the uncompatibilized TPVNs with that of the compatibilized series. Figure 7(a,b) shows the images of samples without staining, and the image shown in Figure 7(c) represents the one in which rubber was stained. The weight ratio of organoclay was 5% in these samples. We observed that for the uncompatibilized TPVNs, most of the organoclay plates appeared as an intercalated bundle and were randomly oriented, whereas the organoclay plates were well dispersed and oriented in a special direction when PPMA was used as a compatibilizer. As shown in Figure 7(c), the organoclays were mostly located at the PP/EPDM interface. This phenomenon suggested that the addition of compatibilizer also tuned the distribution of clay in the polymer bends.[15,19]

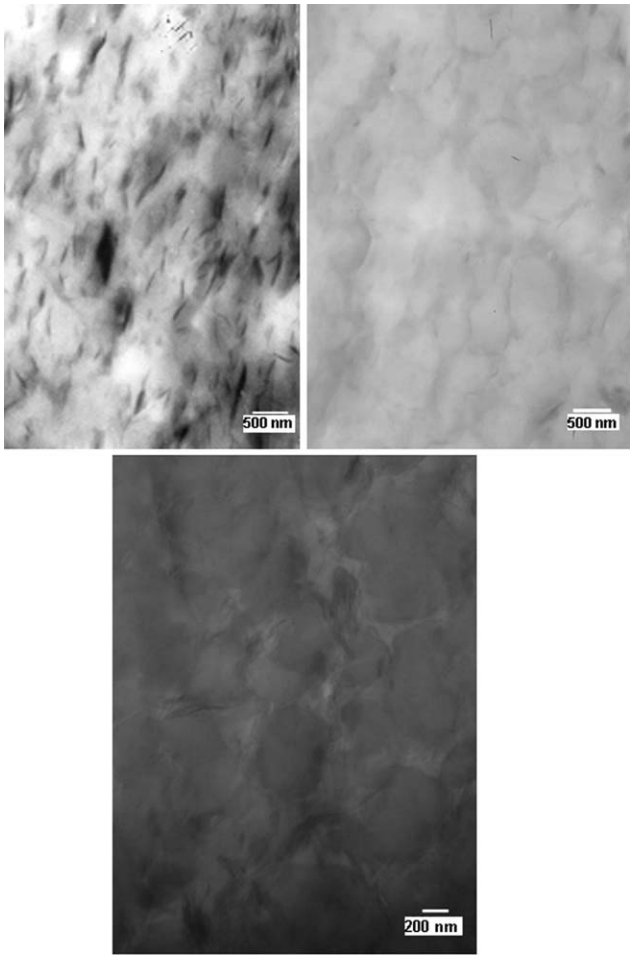

Figure 7. TEM micrographs of the TPVNs: (a) uncompatibilized, (b) compatibilized, and (c) compatibilized and stained.

Dynamic Mechanical Analysis

Figure 8 shows the glass-transition temperatures (T_g's) of the EPDM phase and the PP phase for the TPV and uncompatibilized TPVNs. The addition of organoclay had a minor effect on the T_g of the PP phase, whereas the T_g of the EPDM phase shifted from −31.8 to −26.8°C when organoclay was incorporated into the composites; this was attributed to higher rubber–clay interaction and the hindered cooperative motion of the EPDM chains in the constrained environment, This could also be considered evidence for the selective localization of the organoclay in the EPDM phase. Moreover, a stronger rubber–clay interaction was proven by the reduction in the damping behavior within the rubber transition temperature.[29]

Figure 9 compares the T_g of the neat TPV (PPMA was added) with those of the compatibilized TPVNs. We found that the

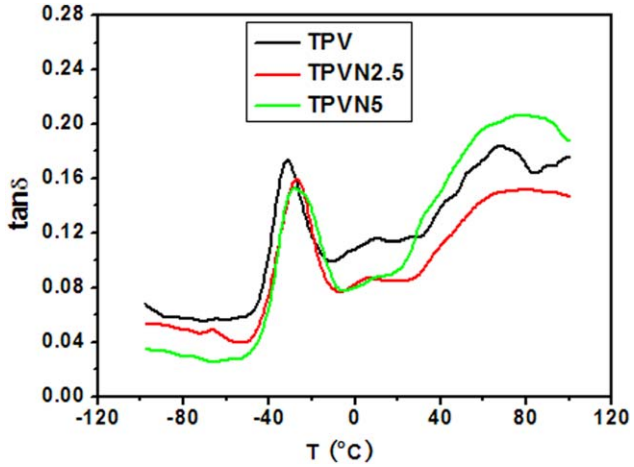

Figure 8. Tan δ values of the uncompatibilized TPVNs as a function of the temperature (T). [Color figure can be viewed in the online issue, which is available at wileyonlinelibrary.com.]

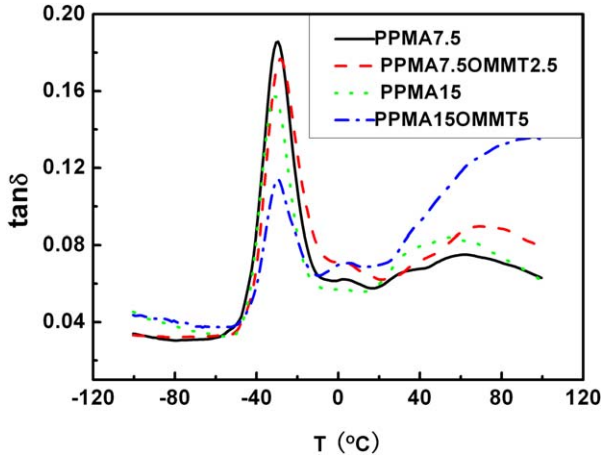

Figure 9. Tan δ of the compatibilized TPVNs as a function of the temperature (The numbers after "PPMA" and "OMMT" represent the content of each component by weight.). [Color figure can be viewed in the online issue, which is available at wileyonlinelibrary.com.]

addition of organoclay had a minor effect on the T_g of the EPDM phase or PP phase. This may have been because the organoclay was mainly distributed at the interface of the PP/EPDM blends, as was illustrated by TEM analysis.

The storage modulus enhancement in the compatibilized TPVNs over that of the pristine counterparts is also shown in Table II. We observed that the compatibilized TPVNs showed modulus enhancement over the temperature range investigated (not shown); this was due to the strengthening effects of the organoclay with a large aspect ratio and the stronger intercalation effects of the polymer chains inside the galleries of the OMMTs. For TPVN5, the modulus enhancement was 72% at 25°C compared to that of its pristine counterpart.

Tensile Properties of the Composites

Table III compares the tensile properties of the prepared samples. The uncompatibilized TPVNs showed an improvement in the mechanical properties compared with those of neat TPV. In comparison with those of neat TPV, the tensile strength of TPVN2.5 increased 30%, and the increase in the elongation at break was 90%. The increase in the tensile properties could be explained by the better dispersion of organoclay in the thermoplastic matrix the relatively strong interaction between the organoclay and matrix through dynamic vulcanization. Although for samples with 5 and 10 wt % OMMT loadings, the tensile strength was lower than the one with 2.5 wt % OMMTs, these changes in the mechanical properties, which should have been due to the excess organoclay loadings, led to a lot of organoclay aggregates in the matrix or at the interface of the two phases.[21] It was interesting to find that the samples of the compatibilized series also showed similar trends in the tensile strength, as shown in Table II. Because the organoclay was not exfoliated, the excess organoclay aggregated, and this led to a decrease in the tensile properties of the samples. However, when it was

Table II. Compositions and Tensile Properties of the TPVNs

	Sample			
PP/EPDM	20/80	20/80	20/80	20/80
OMMT		2.5		5
PPMA	7.5	7.5	15	15
Tensile modulus (MPa)	48	60	75	131
Tensile strength (MPa)	18.6	28.9	26.3	24.3
Elongation at break (%)	450	790	605	660
Storage modulus at 25°C (Pa)	25.9×10^7	31.6×10^7	40.7×10^7	70.0×10^7

Table III. Tensile Properties of the Uncompatibilized TPVNs

Sample	TPV	TPVN1	TPVN2.5	TPVN5	TPVN10	TPVN5 (two-step)
Tensile strength (MPa)	23.5	27.0	30.5	29	27.5	33.5
Tensile modulus (MPa)	54	52	49	62	75	62
Elongation at break (%)	530	720	890	920	860	930

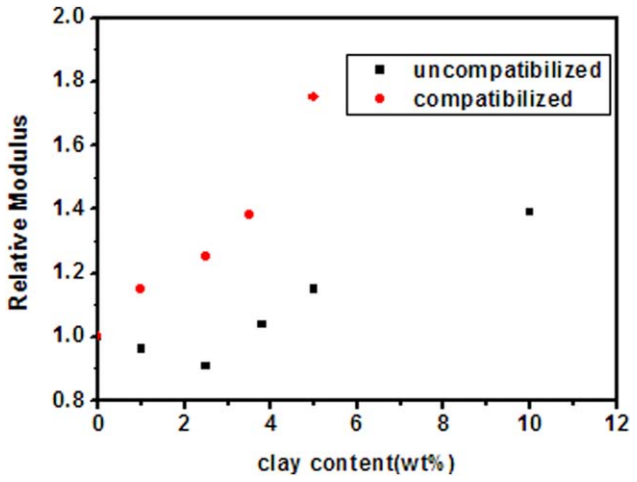

Figure 10. Modulus comparison of the TPVNs. [Color figure can be viewed in the online issue, which is available at wileyonlinelibrary.com.]

prepared with the two-step processing method for uncompatibilized TPVNs, the organoclay preferentially distributed in the rubber phase, and it was selectively reinforced. Thus, TPVN5 prepared with the two-step processing method showed a significant tensile strength enhancement.

Moreover, when compatibilizer was added, the TPVNs nanocomposites showed a more significant increase in the tensile modulus with increasing organoclay concentration; this was because the addition of compatibilizer helped lead to a better intercalation of polymer chains inside the galleries of the organoclay (Figure 10). In addition, the elongation at break of both the uncompatibilized TPVNs and compatibilized series showed moderate increases (see Tables II and III). These results indicate that whether compatibilizer was added or not, an increase in the toughness was achieved when organoclays were incorporated into the composites.

CONCLUSIONS

The morphology of the nanocomposites composed of organoclay and TPV based on uncompatibilized or compatibilized PP/EPDM blends were studied. For the uncompatibilized TPV series, the curing agent had relatively strong interactions with the clay surface and helped the dispersion of the organoclay in the matrix. The organoclay preferred to distribute in the EPDM phase. Also, the rubber particles became larger and were elongated when the organoclay loading was increased. However, for the compatibilized TPV series, the dispersion and distribution of organoclay were controlled by the compatibilizer instead of the curing agent, and the organoclay was dominantly distributed in the interface of PP/EPDM. Moreover, the samples of the uncompatibilized TPV series showed an improvement in the tensile strength compared with that of the neat TPV, although for samples of the compatibilized TPV series, the tensile modulus increased dramatically.

ACKNOWLEDGMENTS

The authors express their sincere thanks to the Initiation Foundation of Hainan University for its financial support (contract grant number kyqd1235).

REFERENCES

1. Coran, A. Y.; Patel, R. P. U.S. Pat. 4,130,535 (**1978**).
2. Coran, A. Y.; Patel, R. P. *Rubber Chem. Technol.* **1980**, *53*, 141.
3. Yin, J. H.; Mo, Z. S.; Ji, F.; Huang, B. T.; Liu, J. Q.; Li, M. X. *Acta Polym. Sin.* **1987**, *4*, 276.
4. Huang, B. T.; Yin, J. H.; Ji, F.; Zhou, E. L.; Mo, Z. S. *Acta Polym. Sin.* **1987**, *4*, 399.
5. Ellul, M. D.; Tsou, A. H.; Hu, W. G. *Polymer* **2004**, *45*, 3351.
6. Goharpey, F.; Katbab, A. A.; Nazockdast, H. *J. Appl. Polym. Sci.* **2001**, *81*, 2531.
7. Winters, R.; Lugtenburg, J.; Litvinov, V. M.; Duin, M.; Groot, H. *J. Polymer* **2001**, *42*, 9745.
8. Meng, X. Y.; Wang, Z.; Zhao, Z. F.; Du, X. H.; Bi, W. G.; Tang, T. *Polymer* **2007**, *48*, 2508.
9. Wang, K.; Liang, S.; Du, R. N.; Zhang, Q.; Fu, Q. *Polymer* **2004**, *45*, 7953.
10. Lee, H. S.; Fasulo, P. D.; Rodgers, W. R.; Paul, D. R. *Polymer* **2005**, *46*, 11673.
11. Maiti, M.; Bandyopadhyay, A.; Bhowmick, A. K. *J. Appl. Polym. Sci.* **2006**, *99*, 1645.
12. Lim, J. W.; Hassan, A.; Rahmat, A. R.; Wahit, M. U. *Polym. Int.* **2006**, *55*, 204.
13. Mishra, J. K.; Hwang, K. J.; Ha, C. S. *Polymer* **2005**, *46*, 1995.
14. Austin, J. R.; Kontopoulou, M. *Polym. Eng. Sci.* **2006**, *46*, 1492.
15. Mehta, S.; Mirabella, F. M.; Rufener, K.; Bafna, A. *J. Appl. Polym. Sci.* **2004**, *92*, 928.
16. Lee, K. Y.; Goettler, L. A. *Polym. Eng. Sci.* **2004**, *44*, 1103.
17. Mishra, J. K.; Ryou, J. H.; Kim, G. H.; Hwang, K. J.; Kim, I.; Ha, C. S. *Mater. Lett.* **2004**, *58*, 3481.
18. Tsai, Y.; Wu, J. H.; Wu, Y. T.; Li, C. H.; Leu, M. T. *Sci. Technol. Adv. Mater.* **2008**, *9*, 1.
19. Naderi, G.; Lafleur, P. G.; Dubois, C. *Polym. Eng. Sci.* **2007**, *47*, 207.
20. Mirzadeh, A.; Lafleur, P. G.; Kamal, M. R.; Dubois, C. *Polym. Eng. Sci.* **2012**, *52*, 1099.
21. Choi, C. H.; Kim, N. Y.; Kim, S. C. *J. Macromol. Sci. Pure Appl. Chem.* **2010**, *47*, 399.
22. Zhao, Z. F.; Tang, T.; Qin, Y. X.; Huang, B. T. *Langmuir* **2003**, *19*, 7157.
23. Gatos, K. G.; Kocsis, J. K. *Polymer* **2005**, *46*, 3069.
24. Das, A.; Costa, F. R.; Wagenknecht, U.; Heinrich, G. *Eur. Polym. J.* **2008**, *44*, 3456.
25. Katbab, A. A.; Nazockdast, H.; Bazgir, S. *J. Appl. Polym. Sci.* **2000**, *75*, 1127.
26. Bazgir, S.; Katbab, A. A.; Nazockdast, H. *J. Appl. Polym. Sci.* **2004**, *92*, 2000.
27. Zheng, H.; Zhang, Y.; Peng, Z. L.; Zhang, Y. X. *Polym. Test.* **2004**, *23*, 217.
28. Gatos, K. G.; Szazdi, L.; Pukanszky, B.; Kocsis, J. K. *Macromol. Rapid Commun.* **2005**, *26*, 915.
29. Li, C. Q.; Zhao, Q. N.; Deng, H.; Chen, C.; Wang, K.; Zhang, Q.; Chen, F.; Fu, Q. *Polym. Int.* **2011**, *60*, 1629.